

9th SYMPOSIUM ON MEASURING TECHNIQUES FOR  
TRANSONIC AND SUPERSONIC FLOWS IN CASCADES  
AND TURBOMACHINES

St. Catherine's College Oxford  
21st - 22nd March, 1988

**DETECTION OF SEPARATION BUBBLES BY HEATED  
THIN-FILM SENSORS IN TRANSONIC TURBINE CASCADES**

F. Kost, W. Bräunling, E. Schüpferling  
DFVLR - Institute for Experimental Fluid Mechanics  
Bunsenstraße 10, D - 3400 Göttingen

R. Göhl  
MTU Motoren- und Turbinen-Union München GmbH  
Dachauer Straße 665, D - 8000 München 50

**Abstract**

Separation bubbles due to the interaction of compression shocks with the suction side boundary layer in a highly loaded gas turbine cascade were detected using heated thin-film sensors. Both the position and the extent of a bubble located like that were compared with results of other measurement techniques like pressure distributions, Schlieren-pictures, oil flow pattern and infra-red images. The agreement was quite good.

First the paper describes the experimental setup. Then the typical output from the heated thin-film sensors in the presence of a separation bubble is shown and some criteria are discussed which allow to discern between the sensor output at a normal boundary layer transition and because of a separation bubble. In contrast to this also the output due to the interaction of a shock and a turbulent boundary layer is shown, where no separation bubble occurred.

## Nomenclature

E	mean output voltage from thin-film anemometer
l	chord length
l <sub>ss</sub>	suction side contour length measured from stagnation point
Ma	Mach number
R	resistance of thin-film sensor
RMS	integrated root mean square value of fluctuating part of output voltage from thin-film anemometer
s	contour length coordinate
t	pitch
$\beta$	flow angle (measured from circumferential direction)
$\beta_s$	stagger angle
Subscripts	
1	measurement plane upstream of cascade
2	homogeneous exit flow from cascade
is	isentropic flow

## Introduction

Aiming towards a better understanding of the flow phenomena in highly loaded turbines, the DFVLR-Institute for Experimental Fluid Mechanics and MTU, München conducted a joint study of a turbine cascade in transonic flow. A cascade equipped with blades especially designed by MTU for transonic flow conditions was investigated in the rectilinear cascade tunnel (EGG) of DFVLR-Göttingen using a variety of measuring techniques, covering conventional pressure measurements, oil flow and schlieren visualization as well as more advanced techniques like thin-film measurements and infrared imaging. This paper, dealing with the heated thin-films, is part of several which summarize the results [1,2]. The measurements were conducted in a large range of flow conditions but this paper confines itself to some flow conditions roughly described by negative and positive incidence angle with one subsonic and one supersonic exit Mach number each.

## Experimental setup

The heated thin-film sensors used were manufactured by MTU. These sensors are vapour deposited onto a foil and this foil was then embedded into the suction surface of the blade. The blades consisted of synthetic resin material and were manufactured by casting in such a way that the foil with the multi-sensor array and the electric connections were flush mounted. The instrumented blade surface of blade 1 was

entirely smooth, blade 2 had a different resin material, perhaps a little bit rougher, in front of the sensors on the blade. The sensor array on one blade was positioned in a staggered way compared to the sensor array on the other blade, such that by measuring with both instrumented blades the time-averaged and the RMS thin-film signal could be obtained at distances of 1.25 mm in flow direction. These blades are shown in **fig.1** and, as can be seen, the thin-films are embedded flush mounted but in a different way into the blade surface. The darker synthetic resin material which is on the whole surface of blade 2 in front of the sensors is rougher than the light resin material of the blade surface elsewhere. The upper part of **fig. 2** gives a sketch of the sensors and the blade surface. A description of the MTU heated thin-film sensors can be found in [3].

In **fig. 2** also the measured resistances of the thin-films at room temperature can be found. As during these measurements no quantitative results were required it seemed to be sufficient to represent all resistances by the mean values indicated in the figure. Furthermore a linear change of resistance with temperature was assumed with a mean factor  $\alpha = 0,0045$  for all sensors. The thin-films were used in the constant temperature mode by connecting them to a DANTEC - anemometer. A description of the measurement procedure can be found in [4,5]. The overheat ratio was chosen constant giving a constant overheat temperature of roughly 115°C of the sensors above the ambient temperature. This overheat temperature cannot be recommended in the future use of this type of sensors as during the measurements some of them were damaged by the high temperature and it was not possible to measure at the same overheat with no flow which would be absolutely necessary when making quantitative measurements. But by choosing such a high temperature it was possible to get very clear output signals and good frequency behaviour of the sensor - anemometer unit.

The DC output voltage of the thin-film anemometer was connected to an integrating digital voltmeter giving the output  $E$  as shown in some of the following figures. The voltage  $E$  in the figures is normalized by  $E_0$ , the anemometer output voltage with no flow, which was however taken at the lower overheat temperature of 60°C. The square of the DC output of the anemometer is proportional to the sum of the heat going into the blade and the heat being convected into the fluid. The heat transfer from the films to the flow is a function of the wall shear stress [6]. Roughly spoken this leads to following behaviour: thin boundary layers above the thin-films will produce higher anemometer voltages  $E$  than thick boundary layers, turbulent boundary layers will produce higher voltages than laminar; in separated zones  $E-E_0$  should be zero or in more qualitative measurements like ours,  $E-E_0$  should at least exhibit a deep minimum in the separated region.

The AC voltage of the thin-film anemometer was stored in a transient recorder which digitized the signal and also computed the RMS-value of the fluctuating signal. During most of our measurements the scanning frequency of the transient recorder was 10 kHz, which means that frequencies up to 5 kHz could be identified. The frequency range is thus of course not sufficient to see turbulent fluctuations, only intermittency or other kind of lower frequency oscillations of the flow can be seen.

### Output from sensors in the presence of a separation bubble

When measuring at negative incidence or more exact at an inlet angle  $\beta_1 = 120.8^\circ$  the suction side boundary layer felt a favourable pressure gradient from the stagnation point up to more than half of the contour length (see **fig. 3**). This meant that the boundary layer remained laminar up to the pressure minimum (see for example the nearly zero AC-voltages in **fig. 10**) and when feeling a pressure rise the laminar boundary layer responded immediately by separating. That is why a separation bubble existed at zero and negative incidence for all Mach numbers from 0.4 to 1.3. This can be most easily proven by making oil flow pictures and **fig. 6** gives an example. But also in the schlieren photos a bubble can sometimes be seen (left column of **fig. 5**) and moreover the bumps in the surface Mach number distributions of **fig. 3** indicate a bubble, too. The thin-film mean voltage curve displays a clear minimum at the location of the bubble (see **fig. 3** and **fig. 8**) but such a minimum would also exist when the boundary layer undergoes a normal transition from laminar to turbulent state without the existence of a separation bubble.

Especially for the subsonic Mach number  $Ma_{2is} = 0.8$  one could not decide from the thin-film signal alone that there exists a separation bubble. For this Mach number the mean voltage signals from the two different blades differ significantly (**fig. 8**). The difference cannot be explained by variations in the thin-film resistance as these are too small for such an effect (see **fig. 2**). A possible explanation is the additional roughness which exists in front of the sensors on blade 2, as explained previously. The RMS-values in **fig. 9** display less differences between the two blades.

In the case of the supersonic exit Mach number  $Ma_{2is} = 1.25$  the mean voltages from the two blades coincide rather well (**fig. 8**), which is perhaps due to the stronger acceleration at this Mach number and seeing the depth of the voltage minimum helps in convincing oneself that there should exist a separation bubble. But using only the information from the thin-film sensors there is a second hint that a separation bubble exists. This is the double peak of the RMS-values in **fig. 9**. A normal boundary layer transition process could not produce such a double peak. But by imagining that the bubble is not really fixed on the blade surface, a sensor at the edge of the bubble will feel a strong variation in the mean value when the bubble moves forward and backward. This means that for example sensors 14 or 18 in **fig. 8** will show strong variations and this is indicated in **fig. 9**, too. Moreover sensor 14 or sensor 20 will show peaks pointing down, when the bubble moves, whereas sensor 15 should display peaks pointing upwards, and sensor 18 should give peaks going up and down. These features of the thin-film AC-voltage can be clearly detected in **figs. 11 and 12**. If an array of sensors is mounted on the blade surface the AC-voltage signal may give the decisive hint whether a separation or normal transition is occurring. During normal transition there should exist first only a few turbulent spots. This means that the sensors lying upstream of transition can only show some peaks which point to higher voltages. At the end of transition there still exist some laminar patches because of the intermittent nature of normal transition. This means that the sensors lying more downstream will display peaks which point to lower voltages when a normal transition process is occurring. So we may infer that the existence of sensor signals displaying downward pointing peaks, followed a little more downstream by sensors display-

ing upward pointing peaks cannot be compatible with normal transition, so then a separation exists.

Being convinced that a separation bubble exists the question arises, whether the boundary layer goes from laminar to turbulent across the bubble. Of course this normally happens. In our case we are convinced that the boundary layer is turbulent after reattachment of the bubble, because, first the mean voltage from the sensors is higher after the bubble than in front of it and second the nearly zero RMS-values existent in the laminar boundary layer (see figs. 9 and 10) do not recur after the bubble. But one cannot decide exactly where the transition happens, whether in the shear layer above the bubble or in the reattachment region.

### Output from sensors in the presence of a purely turbulent boundary layer

At an inlet angle of  $\beta_1 = 155^\circ$ , which means strong positive incidence, a heavy separation can be seen in the schlieren photo (fig. 5, right column). From the oil flow pictures (fig. 7) and the Mach number distributions (fig. 4) it is clear that at the nose of the profile a separation bubble exists, the flow reattaches turbulent shortly behind separation. So the thin-film sensors, the first of them positioned at the normalized contour length of 0.6, are all exposed to a turbulent boundary layer.

At the subsonic exit Mach number  $Ma_{2is} = 0.8$  nothing exciting happens (fig. 4 and 13): No bubble is existing (see fig. 7, top left) and as expected the mean voltage of the sensor is declining after the pressure minimum, from whereon the turbulent boundary layer thickens (fig. 4). The RMS-value remains more or less constant (fig. 13). It should be stated, by the way, that the RMS-values of fig. 13 and fig. 9 cannot be compared quantitatively as at  $\beta_1 = 120.8^\circ$  the scanning frequency of the transient recorder was different from the scanning frequency during the rest of the measurements.

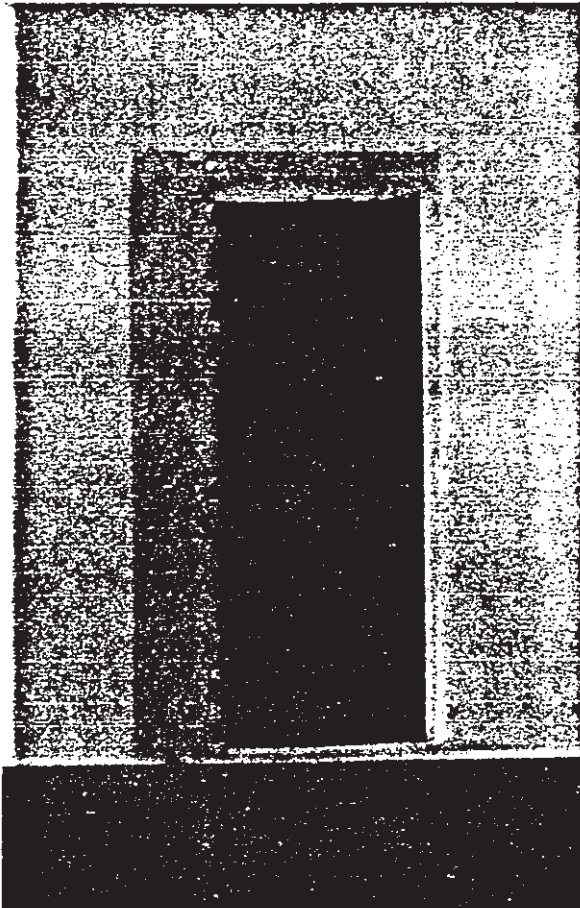
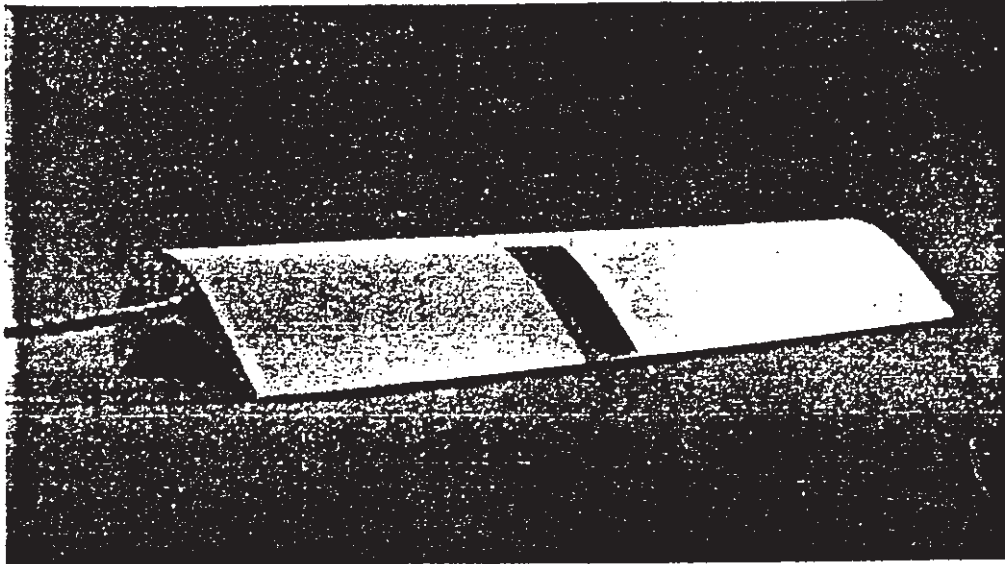
At the supersonic exit Mach number  $Ma_{2is} = 1.25$  the shock from the trailing edge of the neighbouring blade (fig. 5, bottom right) now hits a turbulent boundary layer in contrast to the case of the inlet angle  $\beta_1 = 120.8^\circ$ . Whereas at negative incidence angle the laminar boundary layer separated upstream of the shock, the now turbulent boundary layer can withstand the pressure rise so that no separation occurs. Nevertheless the footprint of the shock can be identified in the oil flow picture (fig. 7, bottom left), at least a thickening of the boundary layer and a considerable local deceleration, which is connected with a local minimum in the shear stress, can be expected [7]. The local shear stress minimum leads to the local minimum in the mean voltage output of the thin-film sensors in fig. 13. So we see again that a local minimum in the output of the sensors cannot automatically be interpreted as transition or a separation bubble. It is necessary to have information from sensors further upstream and downstream so that at least the boundary layer state in front of a local phenomenon is known. The RMS-values in fig. 13 show for the supersonic Mach number a marked peak just at the position of the shock. It is known from instationary schlieren measurements at these blades that the shock itself is oscillating, an effect which can be suppressed by guiding the flow behind the trailing edge of the top blade in the cascade using a plate commonly called 'tailboard' [8].

## Conclusions

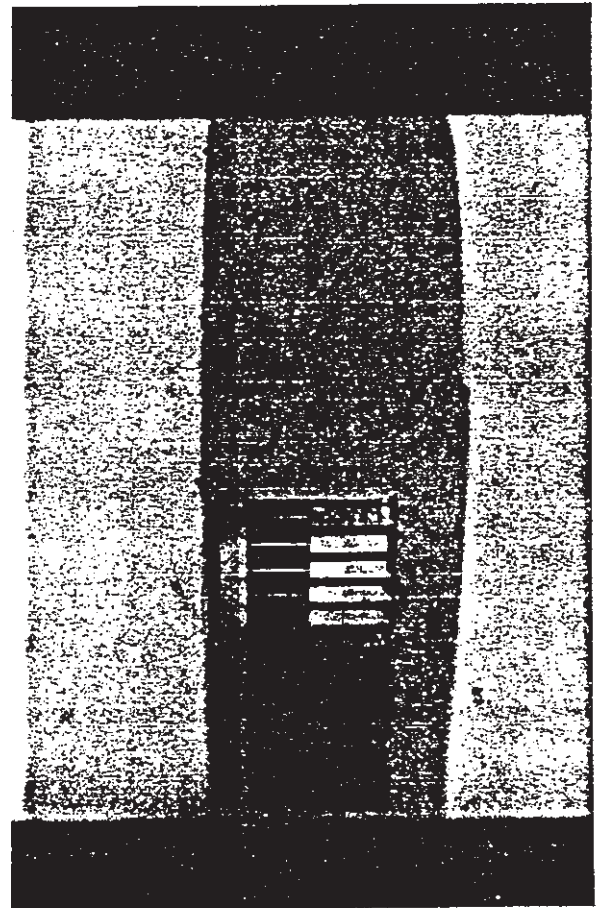
The qualitative measurements described here, show that thin-film measurements are now a valuable tool in fluid mechanics. In conjunction with conventional measurement techniques they give a clear picture of the flow near the blade surfaces. Especially boundary layer state and change of state can be identified more reliably from thin-film measurements than from other surface-bound measurements, mostly because the thin-film output can be splitted into the mean voltage and the fluctuating part and both can be interpreted separately. Moreover the thin-films can also deliver quantitative values of heat transfer and shear stress [5,6], but this normally requires a careful calibration of the sensors.

## References

- [1] Bräunling, W.; Quast, A.; Dietrichs, H.-J.  
"Detection of Separation Bubbles by Infrared Images in Transonic Turbine Cascades"  
ASME paper 88-GT-33 (1988)
- [2] Dietrichs, H.-J.; Hourmouziadis, J.; Malzacher, F. and Bräunling, W.  
"Flow Phenomena in Transonic Turbine Cascades. Detailed Experimental and Numerical investigation",  
Proceedings of the 8th International Symposium on Air Breathing Engines (ISABE), Cincinnati, Ohio, USA (1987)
- [3] Pucher, P.; Göhl, R.  
Experimental Investigation of Boundary Layer Separation with Heated Thin-Film Sensors  
ASME paper 86-GT-254
- [4] Description of the DISA 55M-system  
DANTEC ELEKTRONIK, DK - 2740 Skovlunde, Denmark
- [5] Meier, H.U.; Kreplin, H.-P.  
Experimental Investigation of the Boundary Layer Transition and Separation on a Body of Revolution  
Z.Flugwiss. Weltraumforsch. 4 (1980), Heft 2, pp. 65-71
- [6] Ludwig, H.  
Ein Gerät zur Messung der Wandschubspannung turbulenter Reibungsschichten  
Ingenieur-Archiv, Band 17, 1949, S. 207
- [7] Delery, J.; Marvin, J.G.  
Shock-wave Boundary Layer Interactions  
AGARDograph No. 280, 1986, pp. 20-23
- [8] Detemple, E.  
private communication



blade 1 seen from downstream



blade 2 from above

Fig 1: Blades instrumented with thin film sensors

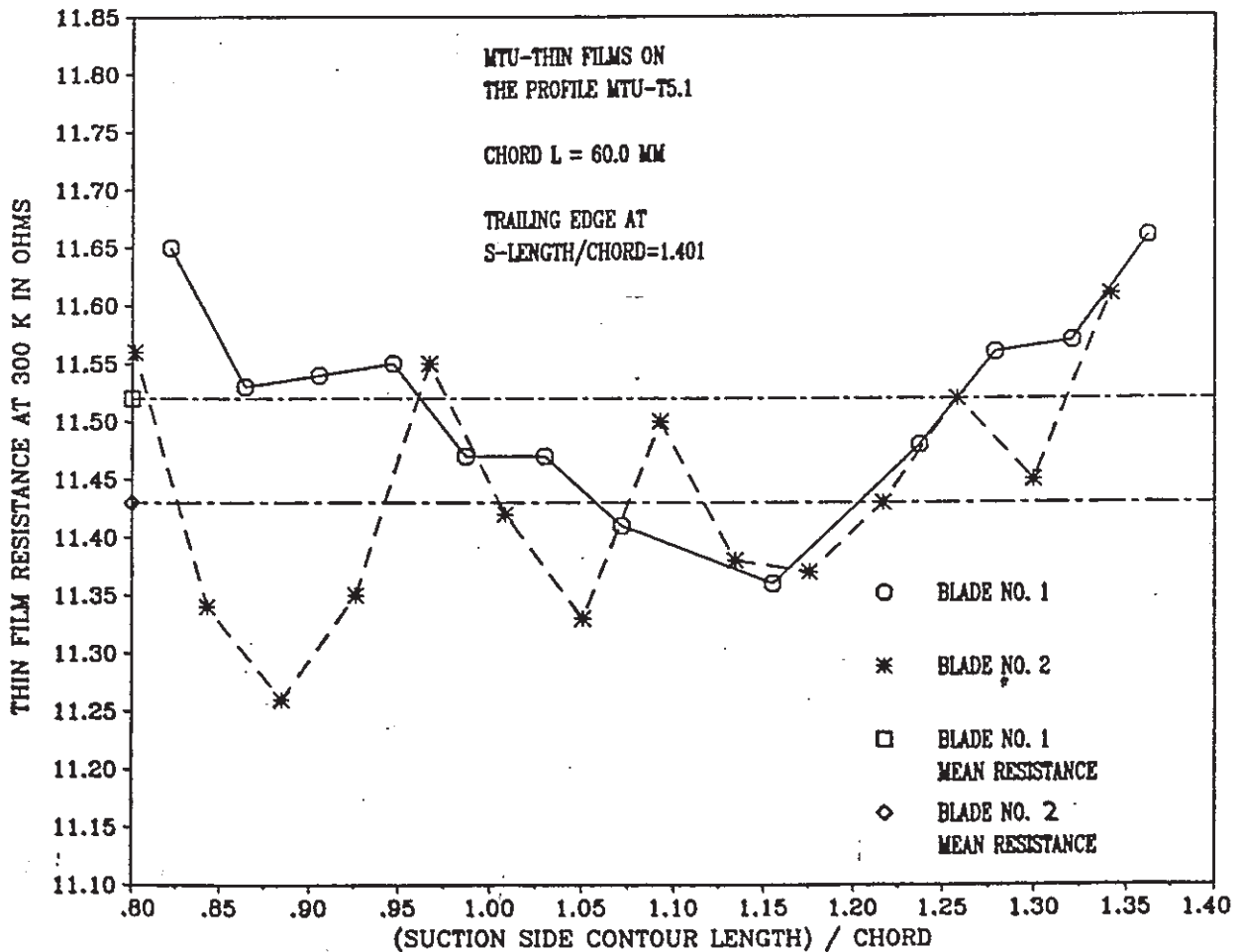
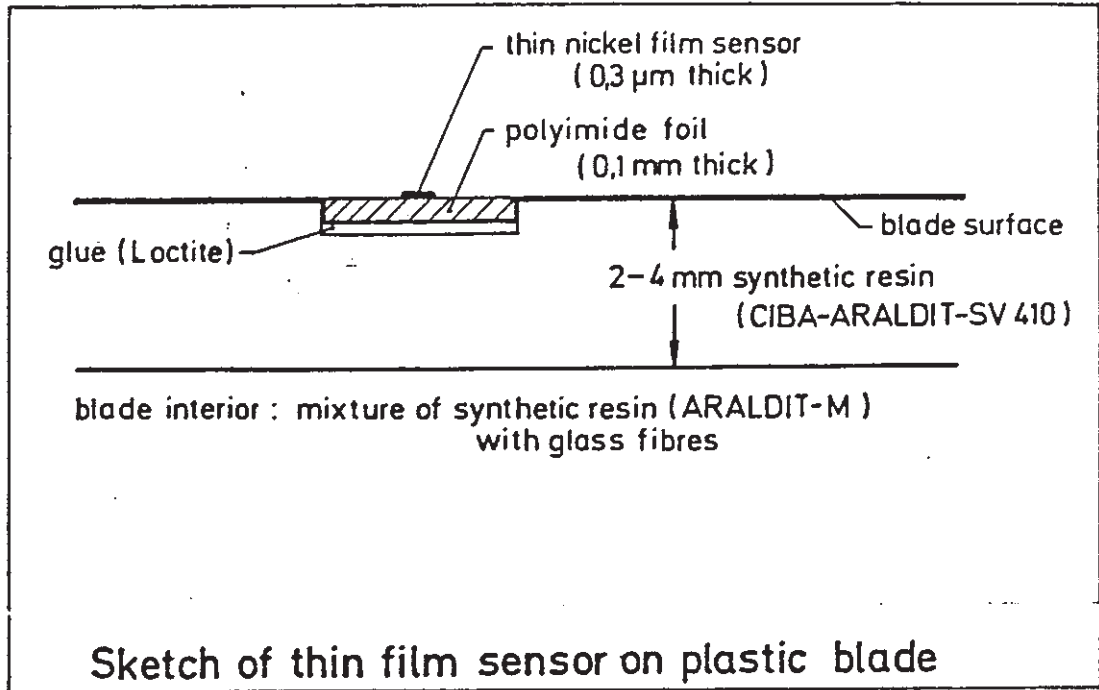


Fig. 2: Sketch of thin film and resistances at room temperature



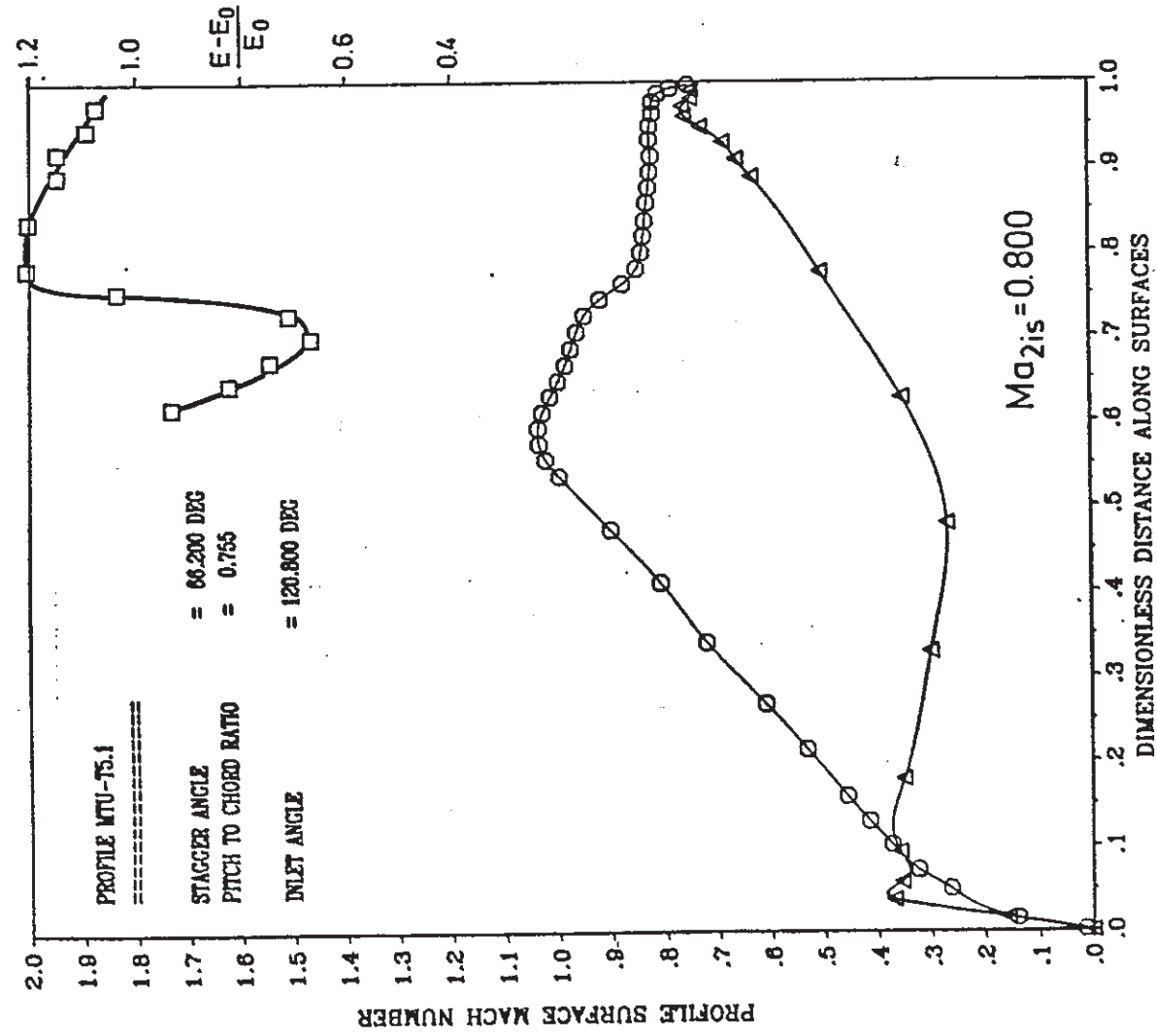
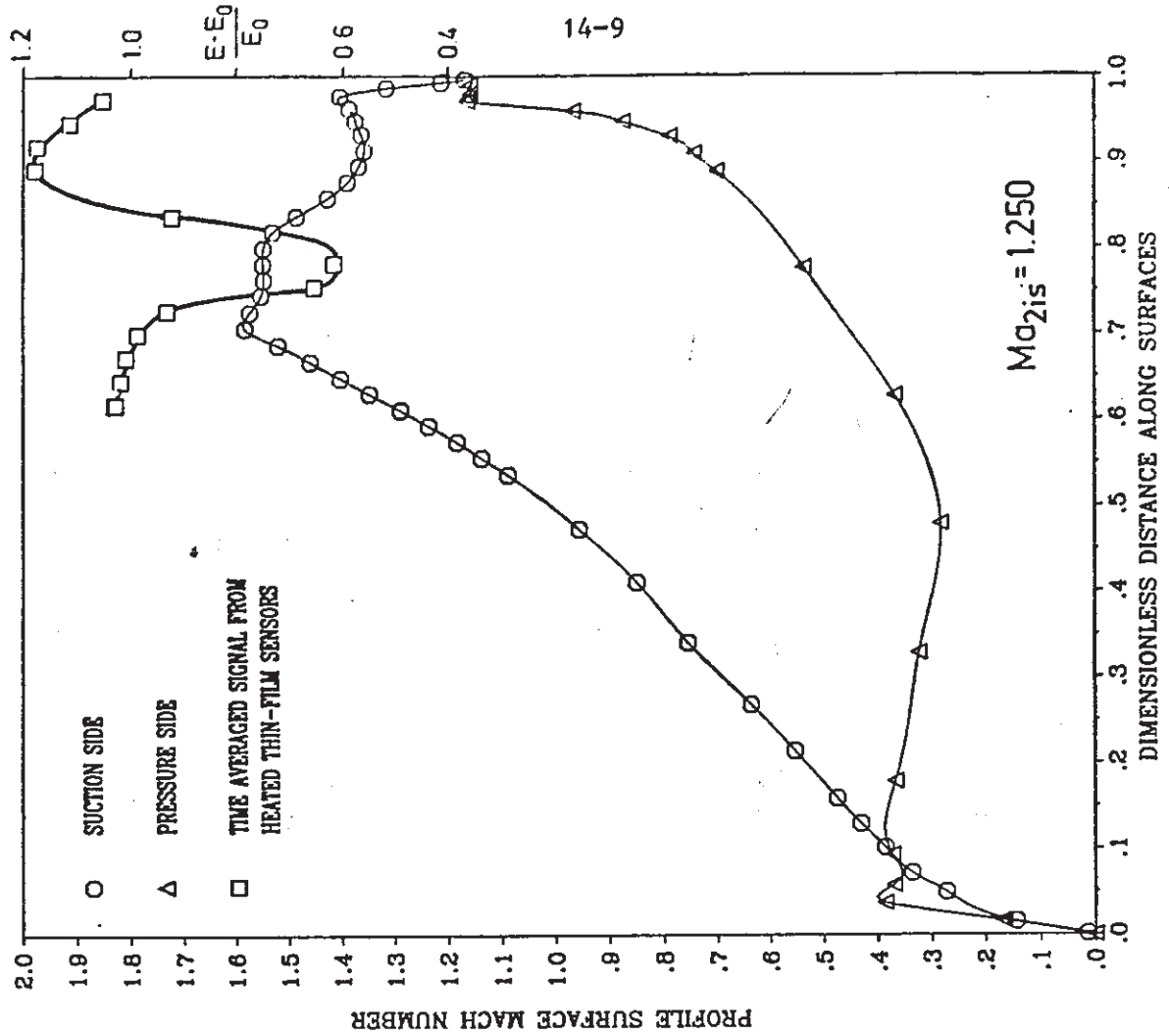


Fig.3: Mach number distribution and thin film voltage at inlet angle 120.8°

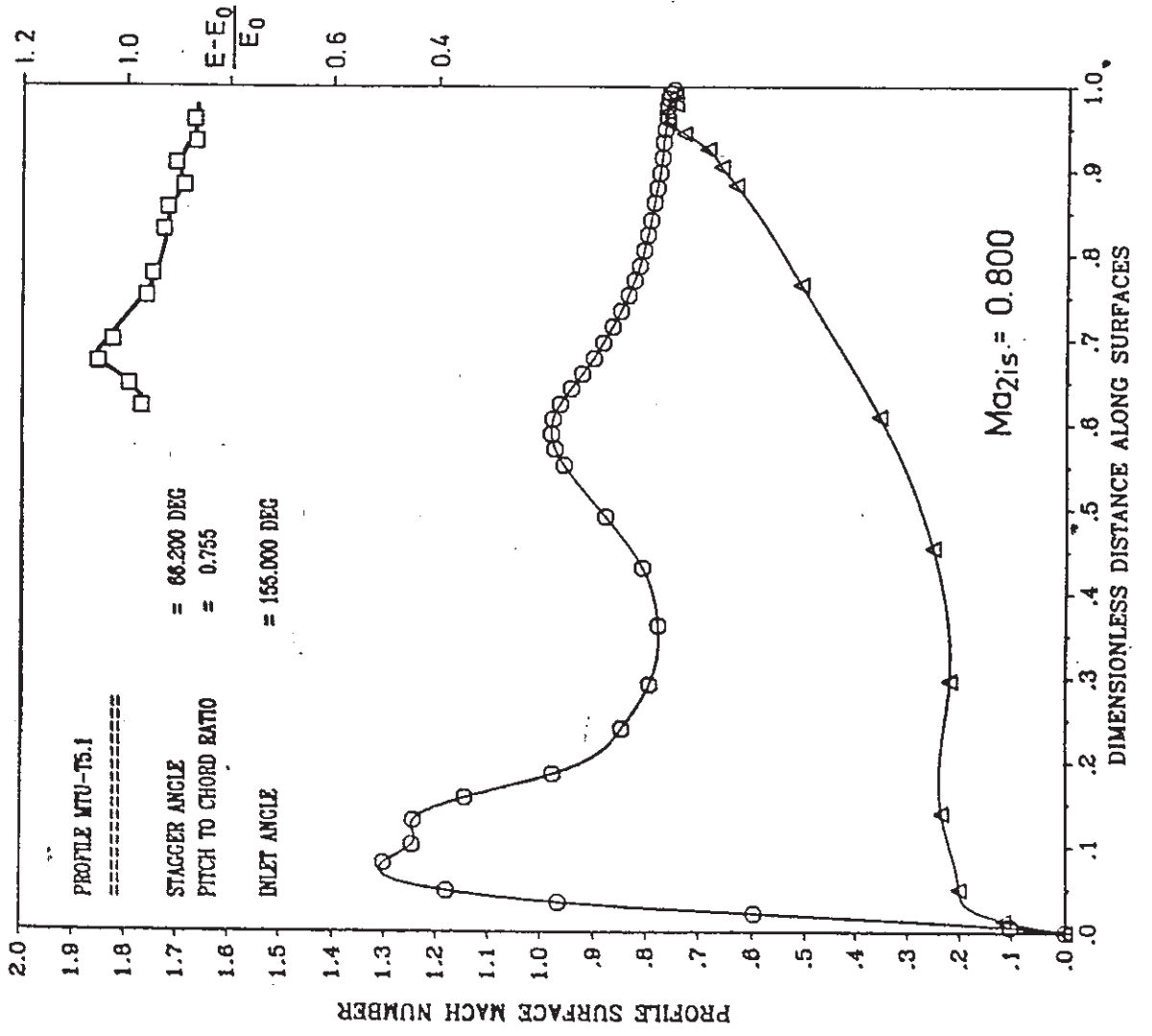
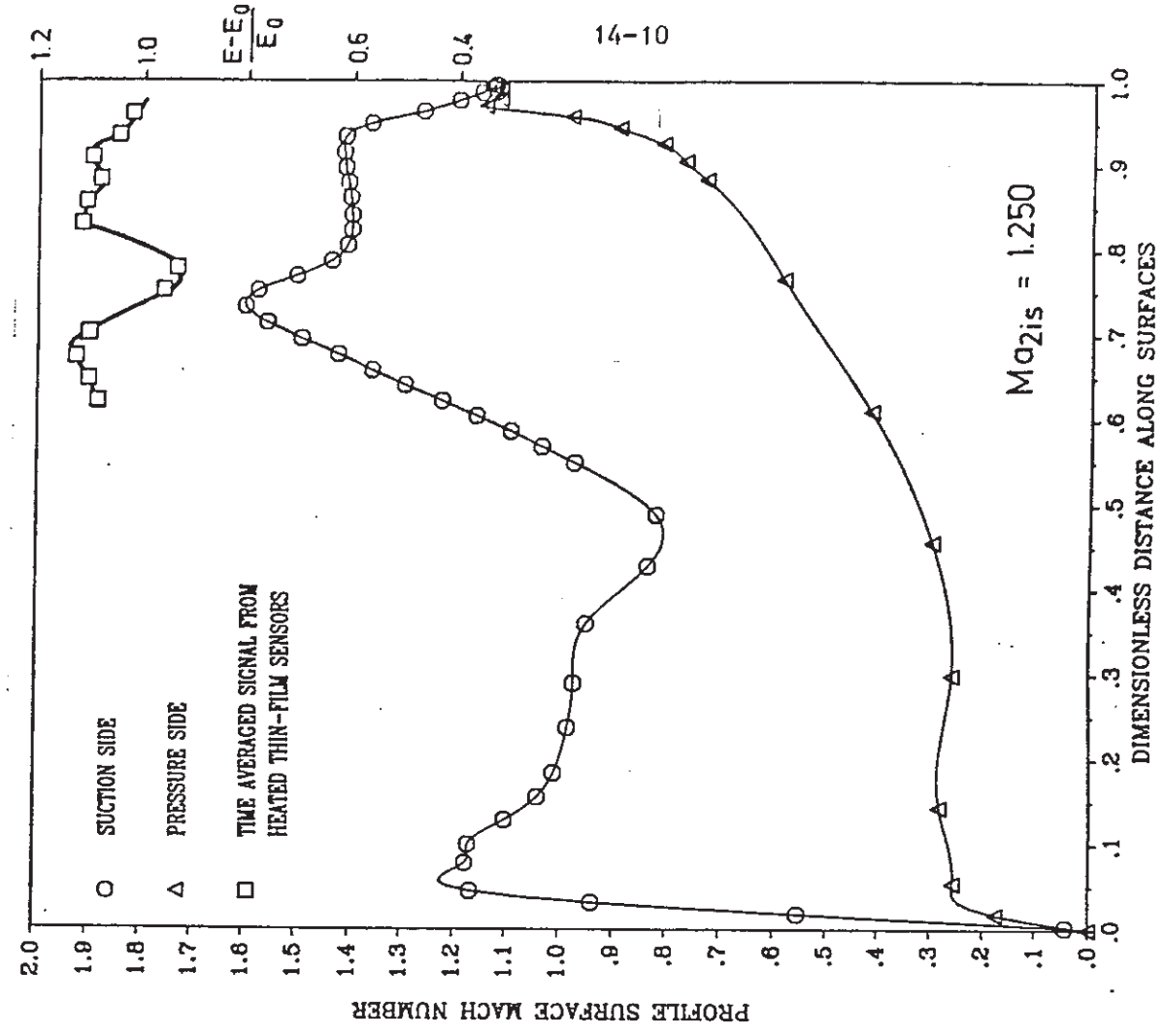
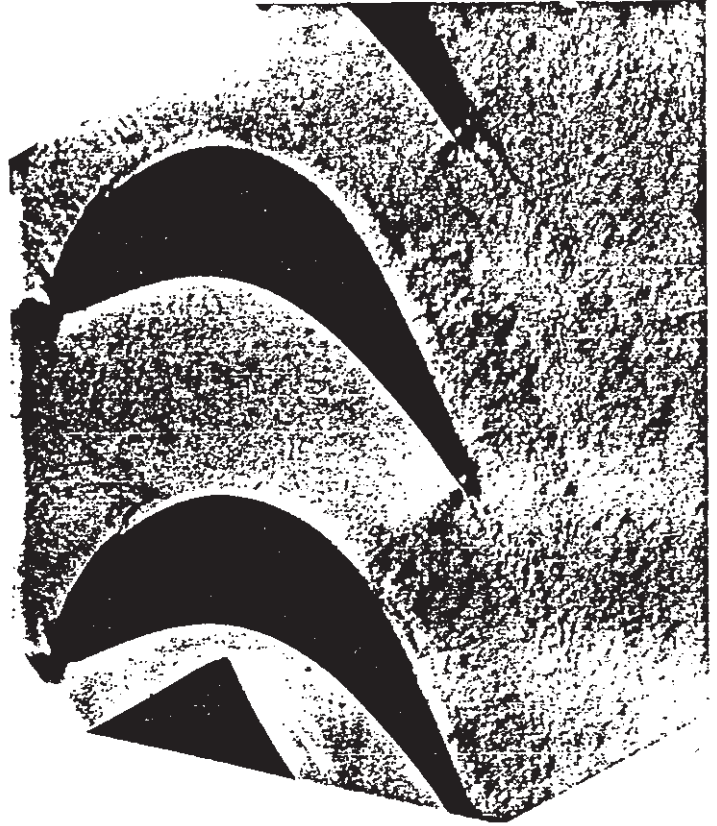


Fig. 4: Mach number distribution and thin film voltage at inlet angle 155°



$$\beta_1 = 120,8^\circ$$

$$Ma_{2is} = 0,80$$



$$\beta_1 = 155,0^\circ$$

$$Ma_{2is} = 0,80$$



$$\beta_1 = 120,8^\circ$$

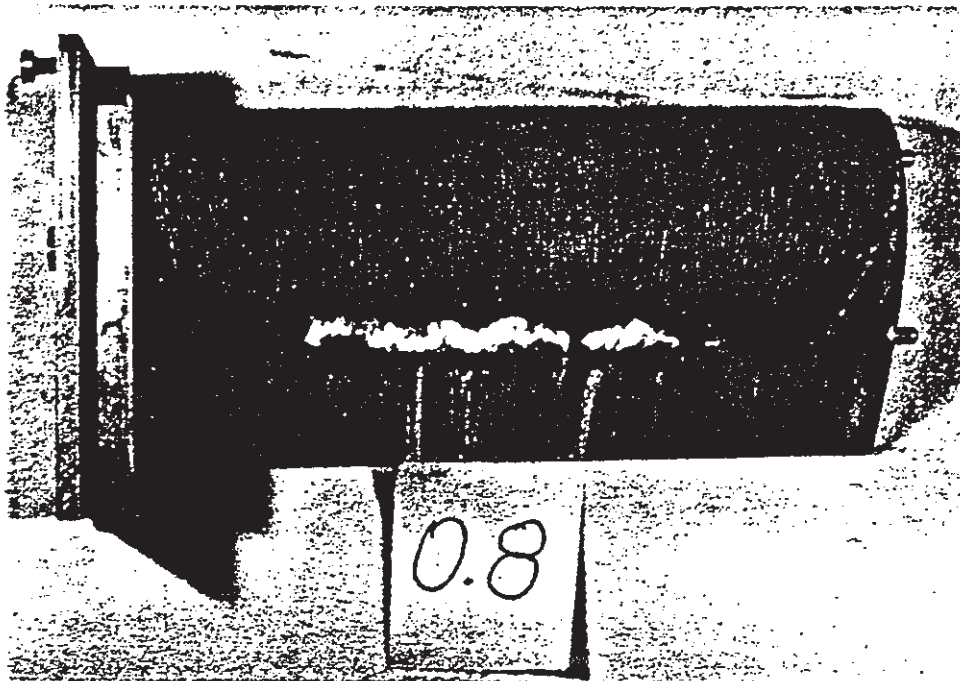
$$Ma_{2is} = 1,25$$



$$\beta_1 = 155,0^\circ$$

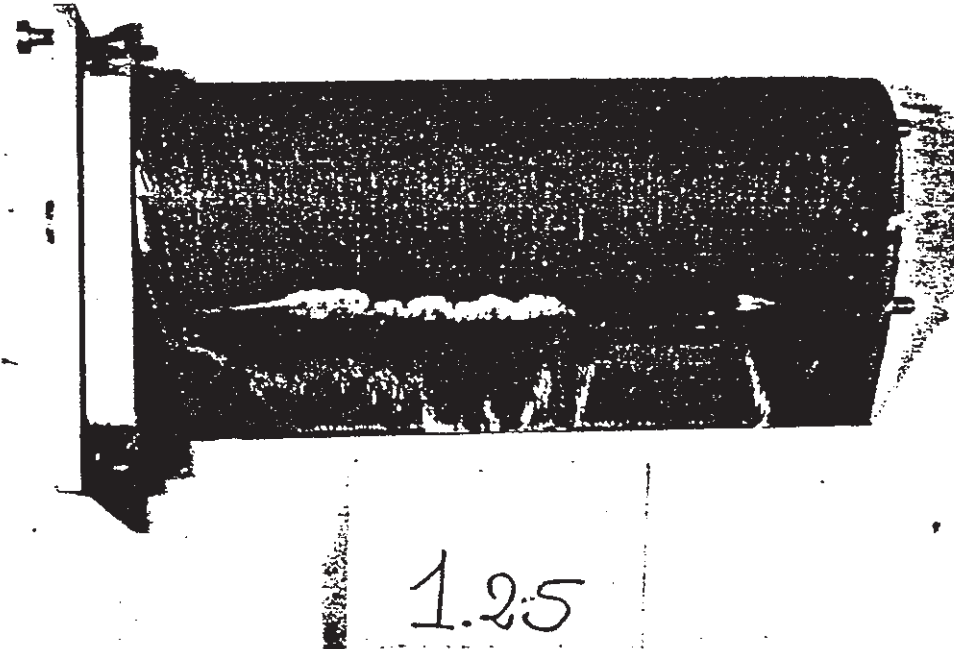
$$Ma_{2is} = 1,25$$

Fig. 5 Schlieren photos profile MTU-T 5.1



$$\beta_1 = 120,8$$

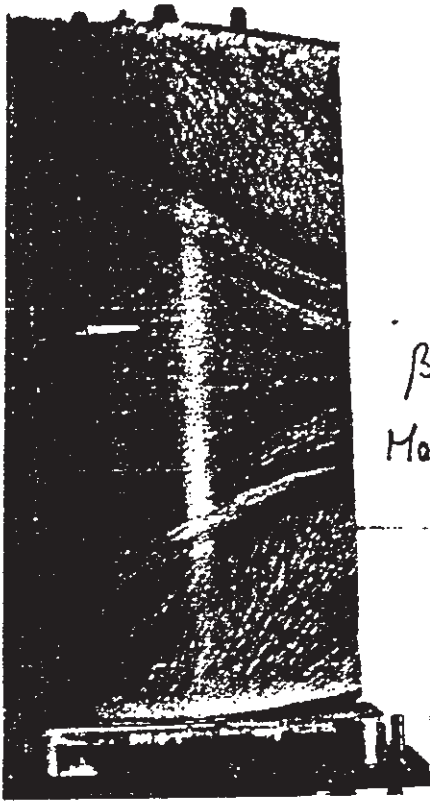
$$Ma_{2is} = 0,80$$



$$\beta_1 = 120,8^\circ$$

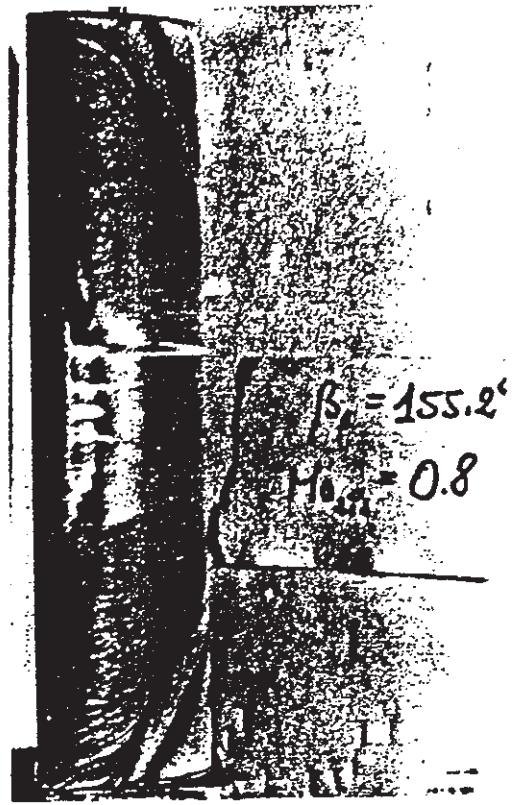
$$Ma_{2is} = 1,25$$

Fig. 6: Oil flow pictures, profiles MTU - T 5.1



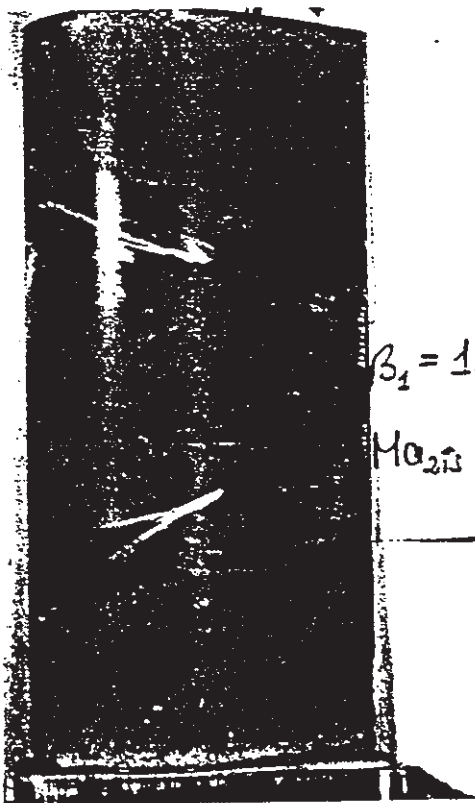
$$\beta_2 = 155.2^\circ$$

$$Mo_{213} = 0.8$$



$$\beta_2 = 155.2^\circ$$

$$Mo_{213} = 0.8$$



$$\beta_2 = 155.2^\circ$$

$$Mo_{213} = 1.25$$

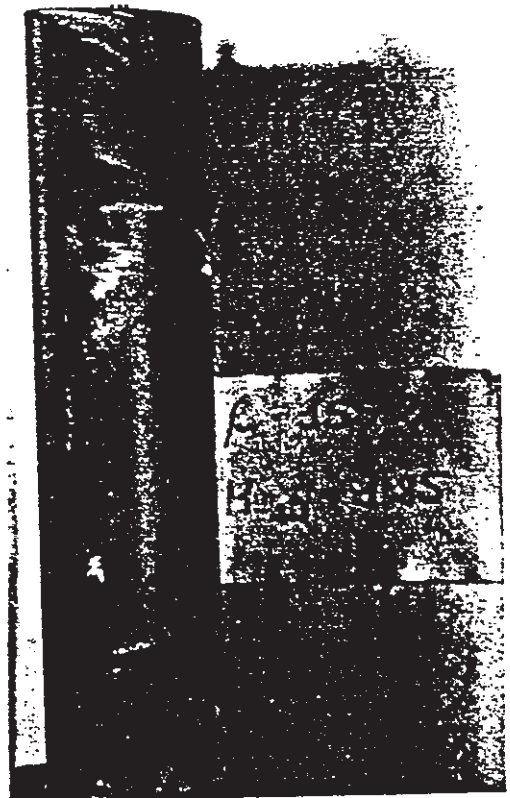


Fig. 7: Oil flow pictures, profiles MTU - T 5.1

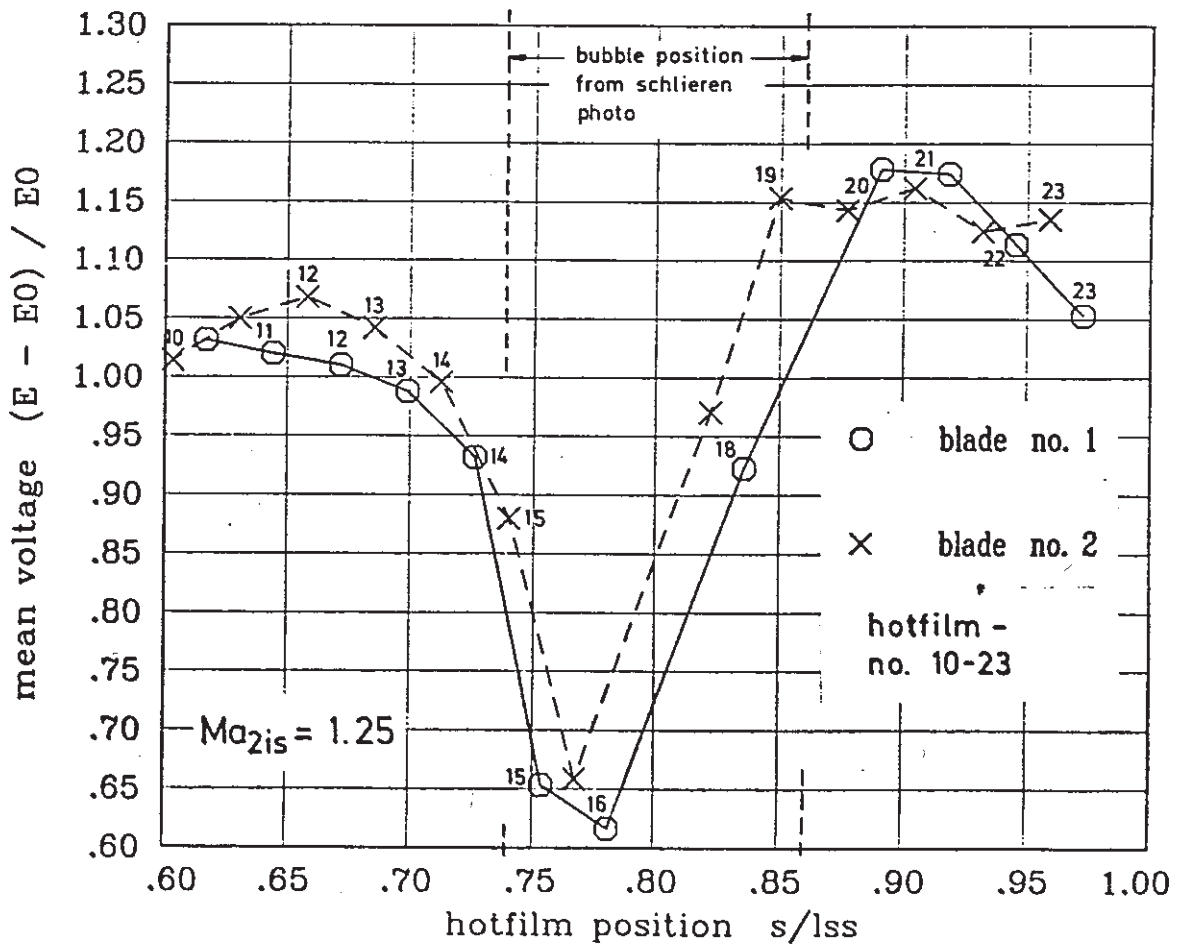
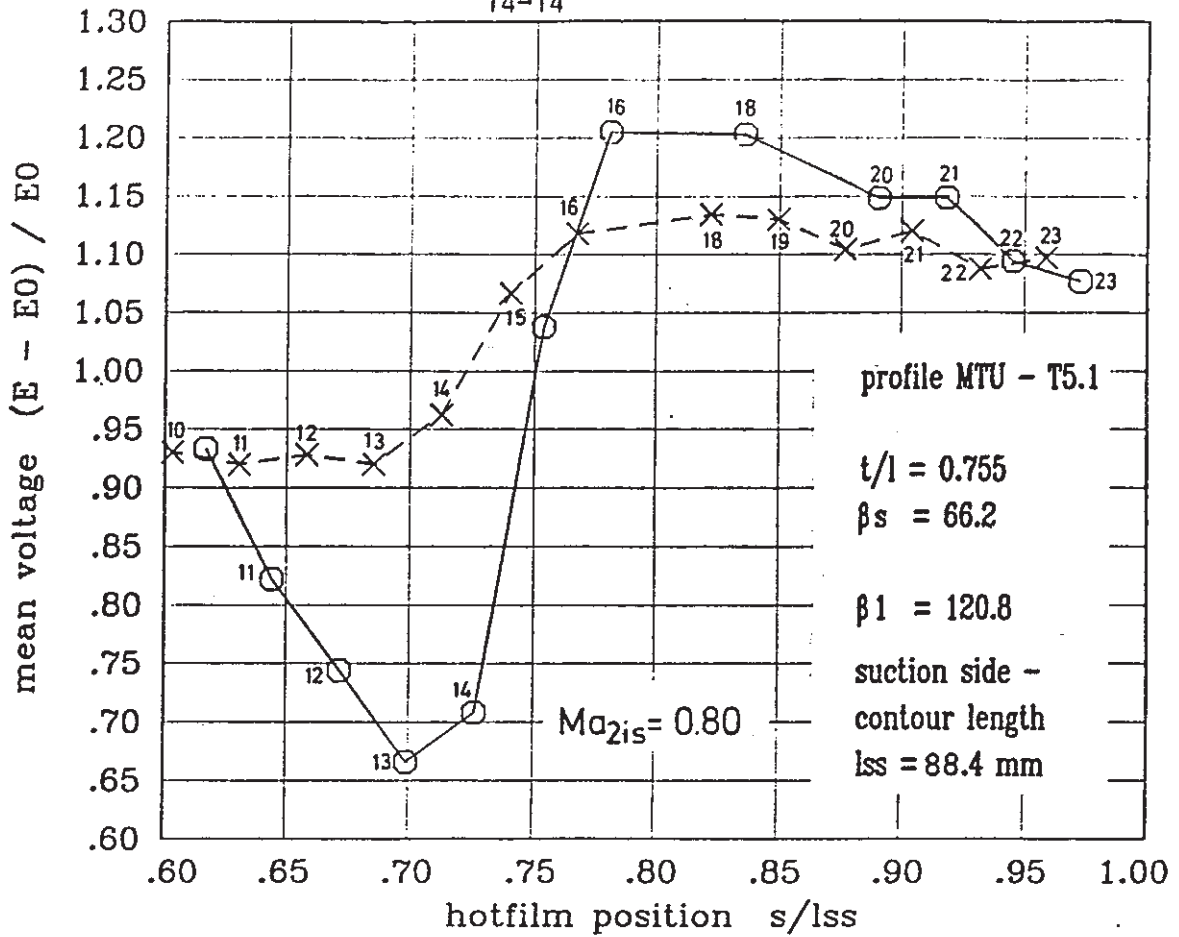
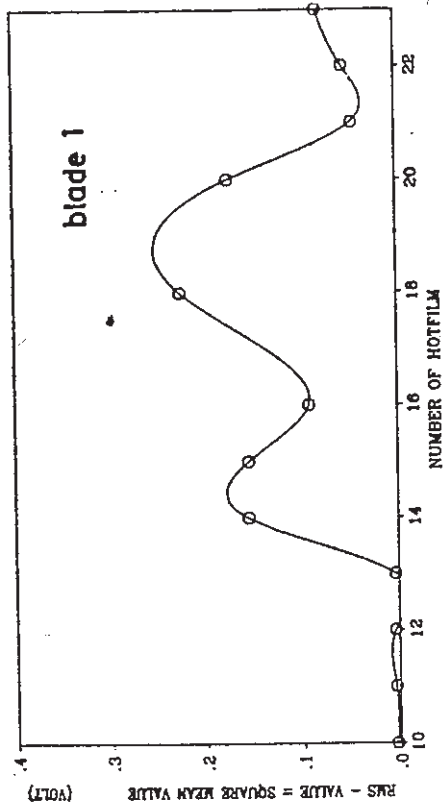


Fig. 8 Sensor mean voltages at inlet angle  $120.8^\circ$

Profil: MTU-T5.1 (1)



Profil: MTU-T5.1 (1)

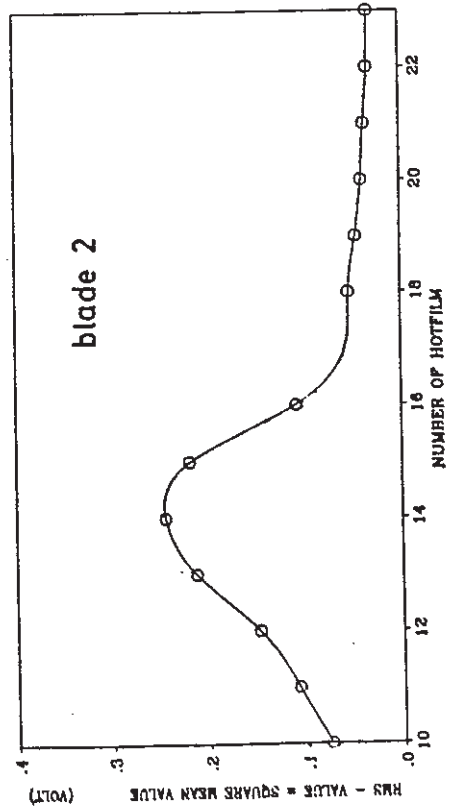
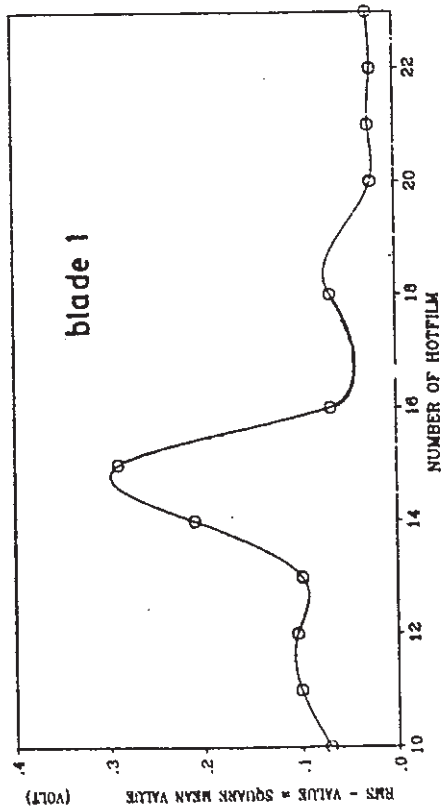
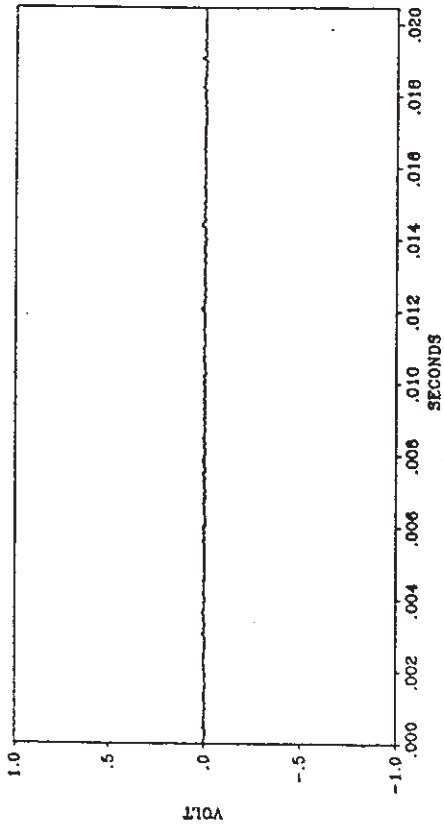
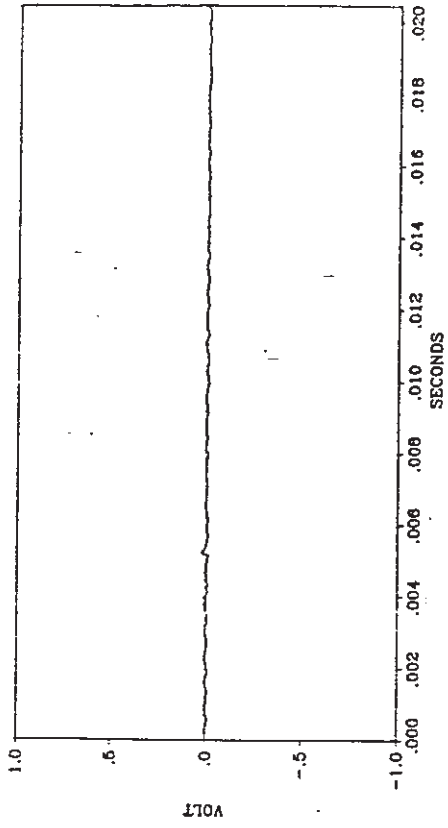


Fig. 9: Sensor RMS-values at inlet angle 120.8°

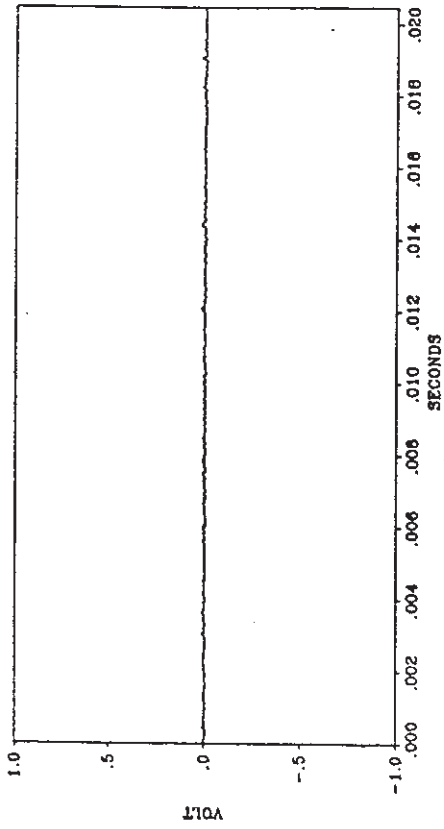
Profil: MTU-T5.1 (1)



Profil: MTU-T5.1 (1)



Profil: MTU-T5.1 (1)



Profil: MTU-T5.1 (1)

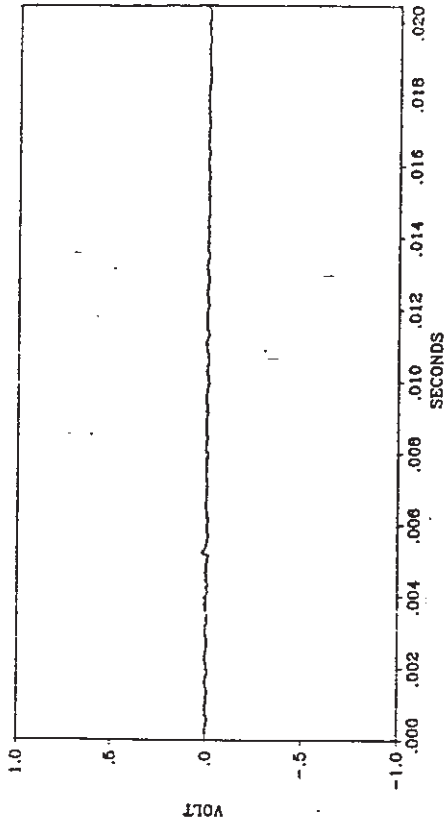
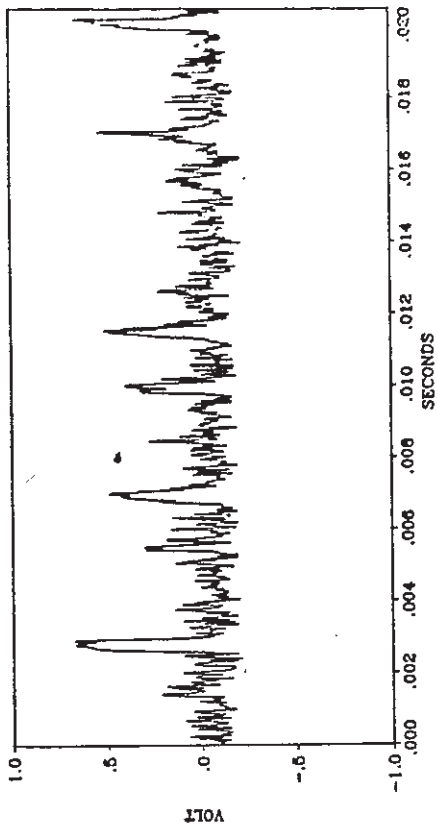


Fig. 10: AC-voltage output for sensors 10-13

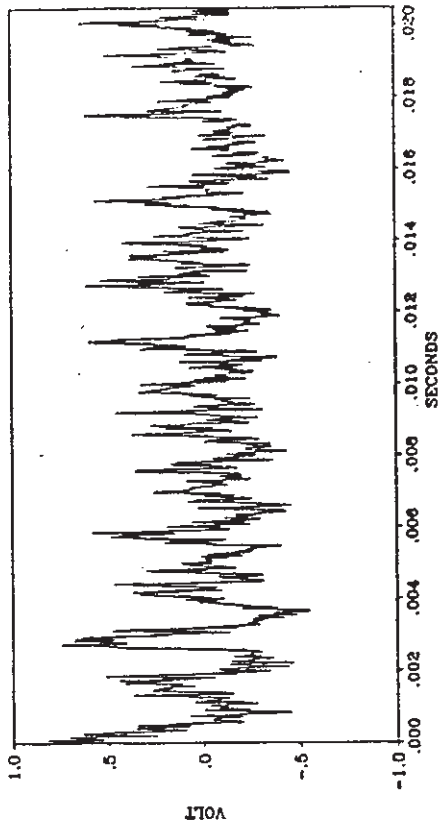


Profil: MTU-T5.1 (1)



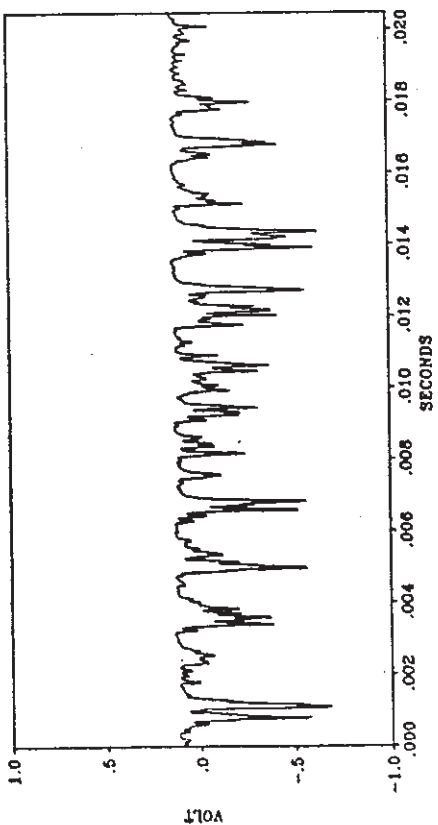
Heißfilm Nr.: 15  
 $\beta_1$ : 120.800  $M_{\text{gas}}$ : 1.250  
 RMS-Wert: .1561

Heißfilm Nr.: 18



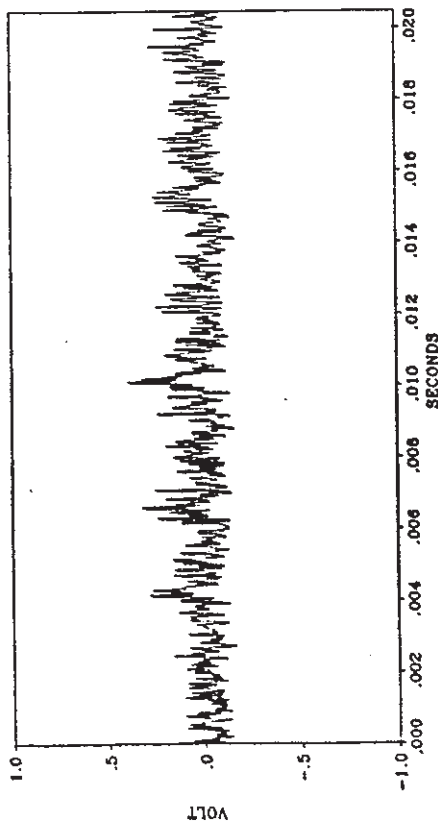
Heißfilm Nr.: 18  
 $\beta_1$ : 120.800  $M_{\text{gas}}$ : 1.250  
 RMS-Wert: .2300

Profil: MTU-T5.1 (1)



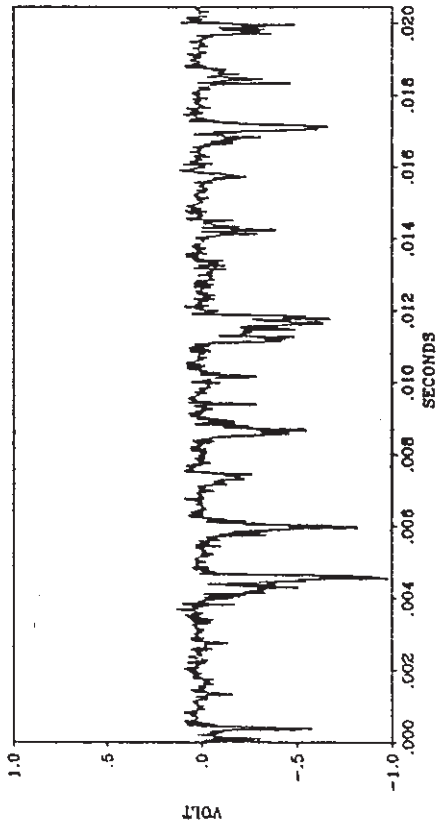
Heißfilm Nr.: 14  
 $\beta_1$ : 120.800  $M_{\text{gas}}$ : 1.250  
 RMS-Wert: .1532

Heißfilm Nr.: 16



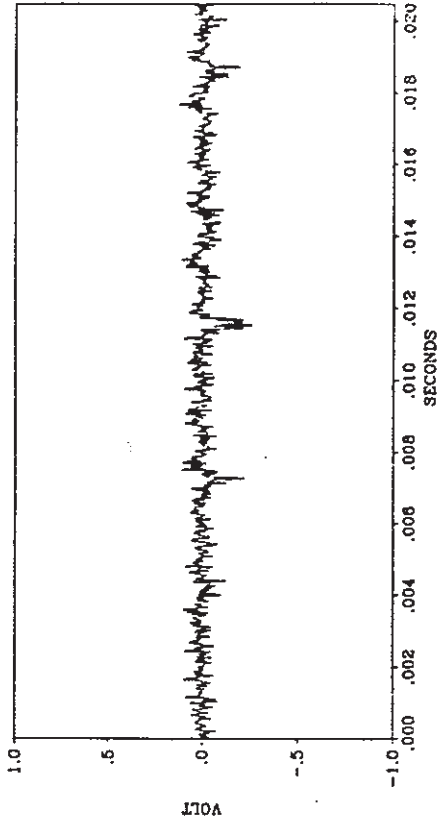
Heißfilm Nr.: 16  
 $\beta_1$ : 120.800  $M_{\text{gas}}$ : 1.250  
 RMS-Wert: .0886

Profil: MTU-T5.1 (1)



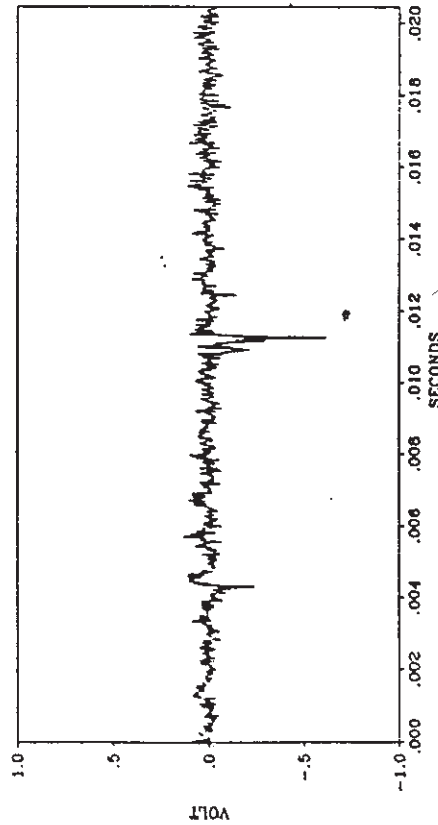
$\beta$ : 120.800 Meas: 1.250  
RMS-Wert: .1621 Heißfilm Nr.: 20

Profil: MTU-T5.1 (1)



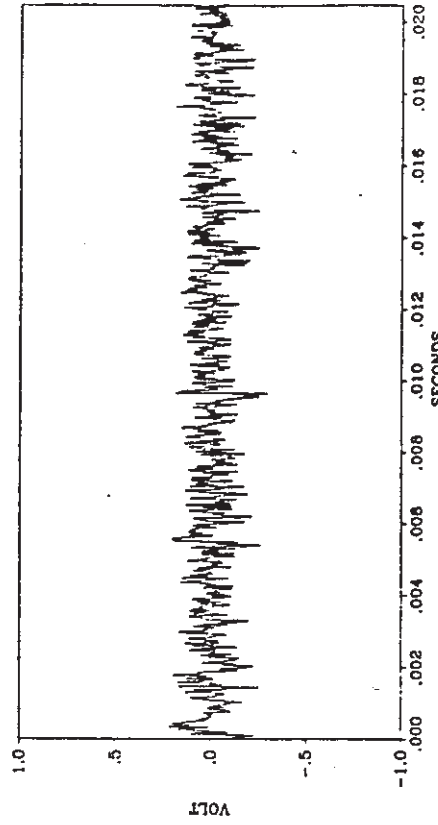
$\beta$ : 120.800 Meas: 1.250  
RMS-Wert: .0436 Heißfilm Nr.: 21

Heißfilm Nr.: 22



$\beta$ : 120.800 Meas: 1.250  
RMS-Wert: .0498

Heißfilm Nr.: 23



$\beta$ : 120.800 Meas: 1.250  
RMS-Wert: .0022

Fig.12: AC-voltage output for sensors 20-23

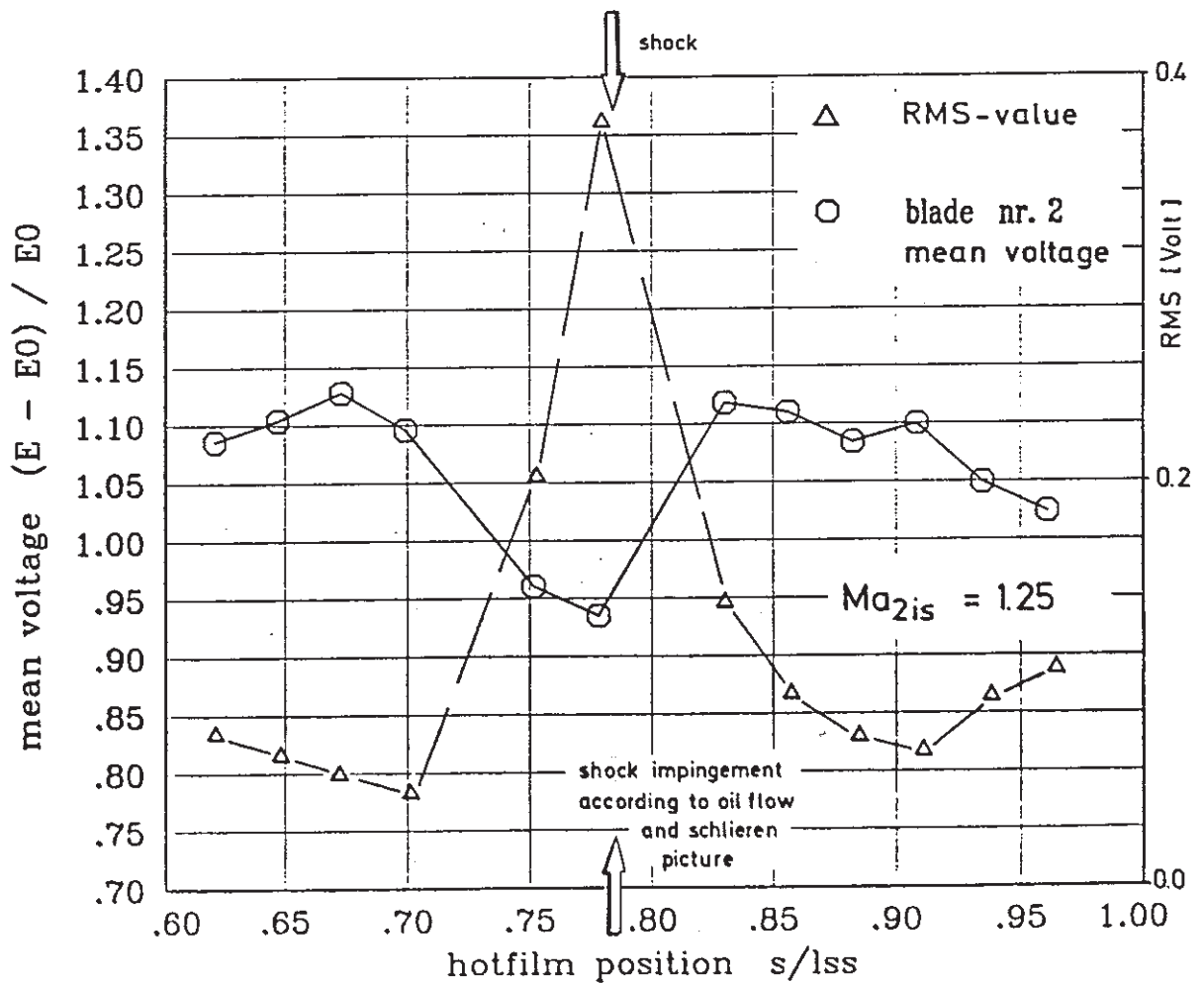
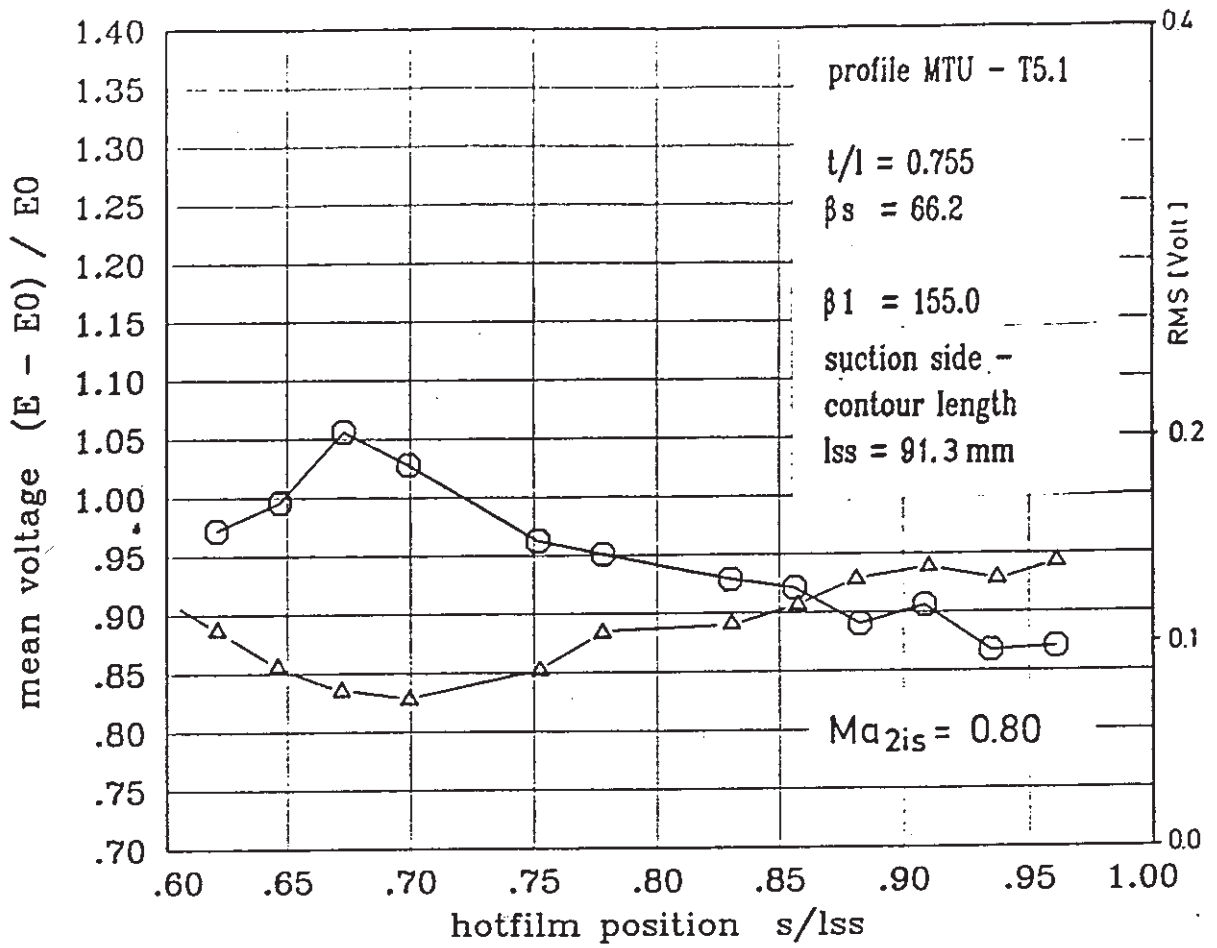


Fig. 13: Sensor mean voltages and RMS-values